Electronic Supplementary Material (ESI) for Dalton Transactions.

Benzothiazole-Pyrimidine-Based BODIPY Analogues: Promising Luminophores with Fluorescence Sensing and Imaging Ability and Asymmetrization-Induced Solid-State Emission

Xiaoqing Wang,[†,a,c] Qingsong Liu,[†,b] Fen Qi,[a,b] Lin Li,[a] Hai-Dong Yu,[a] Zhipeng Liu*[a,b] and Wei Huang*[a,d]

[a] Key Laboratory of Flexible Electronics (KLOFE) & Institute of Advanced Materials (IAM), Jiangsu National Synergetic Innovation Center for Advanced Materials (SICAM), Nanjing Tech University (NanjingTech), 30 South Puzhu Road, Nanjing, 211816, P.R. China. E-mail: iamzpliu@njtech.edu.cn (Z.L.); iamwhuang@njtech.edu.cn (W.H.).

[b] Institute of Functional Organic Molecules and Materials, School of Chemistry and Chemical Engineering, Liaocheng University, No.1 Hunan Road, Liaocheng, 252000, P.R. China.

[c] Institute of Advanced Synthesis (IAS), Nanjing Tech University (NanjingTech), 30 South Puzhu Road, Nanjing, 211816, P.R. China.

[d] Key Laboratory for Organic Electronics and Information Displays & Institute of Advanced Materials (IAM), Jiangsu National Synergetic Innovation Center for Advanced Materials (SICAM), Nanjing University of Posts & Telecommunications, 9 Wenyuan Road, Nanjing 210023, P.R. China.

[†] Both authors contribute equally to this work.

1. Synthesis[1]

General. All reactions and manipulations of air-sensitive compounds were carried out under dry argon by using Schlenk techniques. Solvents were dried prior to use by common methods in organometallic chemistry. Chemicals were commercially obtained and used as received. ^{1}H and ^{13}C NMR spectra were recorded using Varian Mercury-plus 400M spectrometer instrument. Chemical shifts are reported in ppm relative to $Si(CH_3)_4$ (^{1}H), and coupling constants (*J*) are given in Hz. Mass spectra were obtained on a LCQ (ESI-MS, Thermo Finnigan) mass spectrometer. Thin layer chromatography (TLC) was performed on plates coated with thick silica gel GF254 (Qingdao Haiyang Chemical Co., Ltd). Column chromatography was performed using silica gel (200 mesh, Qingdao Haiyang Chemical Co., Ltd).

*General procedure for the synthesis of compounds **1** and **2**.*

To a stirred suspension of NaH (60 w% in oil, 5.0 equiv..) in dry THF was added a solution of 2-(benzo[*d*]thiazol-2-yl)acetonitrile (1.0 equiv.) in dry THF dropwise. After the mixture was stirred 0.5 h at room temperature, a solution of 2,4-dichloropyrimidine or 4,6-dichloropyrimidine (1.1 equiv.) in dry THF was added dropwise, and the resulting mixture was heated to reflux for 24 h. Then 2 M HCl aq. was slowly added and the yellow precipitate was filtered and washed with water. After drying, the desire product was obtained.

---

[1] Due to the poor solubility of **BDB1-8** in common organic solvents, their ^{13}C NMR spectra were not obtained.

*Compound **1***. Yield: 80%, ^{1}H NMR (400 MHz, $CDCl_3$) δ/ppm = 13.48 (s, 1H), 8.36 (d, *J* = 5.6 Hz, 1H), 7.68 (d, *J* = 7.9 Hz, 1H), 7.49 (d, *J* = 6.4 Hz, 2H), 7.34 (t, *J* = 7.1 Hz, 1H), 7.18 (d, *J* = 5.6 Hz, 1H).

*Compound **2***. Yield: 90%, ^{1}H NMR (400 MHz, $CDCl_3$) δ/ppm = 15.45 (s, 1H), 8.17 (d, *J* = 5.8 Hz, 1H), 7.84 (t, *J* = 6.0 Hz, 1H), 7.74 – 7.64 (m, 1H), 7.50 (d, *J* = 9.0 Hz, 1H), 7.15 (d, *J* = 5.8 Hz, 1H), 6.79 (t, *J* = 6.6 Hz, 1H).

*General procedure for the synthesis of **BDB1** and **BDB2**.*

To a CH_2Cl_2 solution containing the compound **1** or compound **2** (1 equiv.) was added DBU (3 equiv.) at room temperature. After stirring for 10 min, BF_3•OEt_2 (5 equiv.) was added dropwise and the reaction was continued for 3 h at room temperature. Then the solution was poured into water and the organic phase was extracted with dichloromethane. The organic layer was dried over magnesium sulfate and the solvent was removed under vacuum. Pure product was then obtained by silica gel column chromatography.

BDB1 was obtained as a bright yellow powder. Yield: 60%. ^{1}H NMR (400 MHz, $CDCl_3$) δ/ppm = 8.21 (d, *J* = 6.0 Hz, 1H), 8.09 (d, *J* = 8.2 Hz, 1H), 7.80 (d, *J* = 8.0 Hz, 1H), 7.60 (t, *J* = 7.9 Hz, 1H), 7.48 (t, *J* = 7.7 Hz, 1H), 7.32 (d, *J* = 6.0 Hz, 1H). HRMS (ESI): calcd., $[M+H]^+$ = 335.0142, found: $[M+H]^+$ = 335.0132.

BDB2 was obtained as a yellow powder. Yield: 65%. ^{1}H NMR (400 MHz, $CDCl_3$) δ/ppm = 8.77 (s, 1H), 8.04 (d, *J* = 8.3 Hz, 1H), 7.80 (d, *J* = 8.0 Hz, 1H), 7.59 (dd, *J* = 12.1, 4.7 Hz, 1H), 7.47 (t, *J* = 7.7 Hz, 1H), 7.38 (s, 1H). HRMS (ESI): calcd., $[M+H]^+$ = 335.0142, found: $[M+H]^+$ = 335.0132.

*General procedure for the synthesis of **BDB3** and **BDB4**.*

To a methanol solution containing the ***BDB1*** or ***BDB2*** (1.0 equiv.) was added sodium methoxide (2.0 equiv.) in methanol dropwise under argon atmosphere, and the resulting mixture was heated to reflux for 8 h. After cooling down to room temperature, the precipitation was filtered and rinsed with cold methanol.

BDB3 was obtained as an offwhite powder. Yield: 88%. ^{1}H NMR (400 MHz, $CDCl_3$) δ/ppm = 8.17 (d, *J* = 5.9 Hz, 1H), 8.04 (d, *J* = 8.3 Hz, 1H), 7.74 (d, *J* = 8.1 Hz, 1H), 7.56 – 7.51 (m, 1H), 7.43–7.37 (m, 1H), 7.02–6.97 (m, 1H), 4.22 (s, 3H). HRMS (ESI): calcd., $[M+H]^+$ = 331.0637, found: $[M+H]^+$ = 331.0639.

BDB4 was obtained as an offwhite powder. Yield: 91%. ^{1}H NMR (400 MHz, $CDCl_3$) δ/ppm = 8.79 (s, 1H), 7.94 (d, *J* = 8.4, 1H), 7.71 (d, *J* = 7.9, 1H), 7.52 (t, *J* = 7.8, 1H), 7.37 (t, *J* = 7.3, 1H), 6.64 (s, 1H), 4.11 (s, 3H). HRMS (ESI): calcd., $[M+H]^+$ = 331.0637, found: $[M+H]^+$ = 331.0645.

*General procedure for the synthesis of **BDB5** and **BDB6**.*

To a CH_2Cl_2 solution containing the ***BDB1*** or ***BDB2*** (1.0 equiv.) was added dimethylamine hydrochloride (2.0 equiv.) and Et_3N (3 equiv.) at room temperature. The reaction was continued for 2 h and then the solution was poured into water and the organic phase was extracted with dichloromethane. The organic layer was dried over magnesium sulfate and the solvent was removed under vacuum.

BDB5 was obtained as a yellow-green powder. Yield: 98%. ^{1}H NMR (400 MHz, $CDCl_3$) δ/ppm = 8.11 (d, *J* = 5.3 Hz, 1H), 8.06 (d, *J* = 8.5 Hz, 1H), 7.71 (d, *J* = 7.9 Hz, 1H), 7.52–7.45 (m, 1H), 7.39–7.32 (m, 1H), 6.73 (d, *J* = 5.3 Hz, 1H), 3.18 (s, 6H). HRMS (ESI): calcd., $[M+H]^+$ = 344.0954, found: $[M+H]^+$ = 344.0955.

BDB6 was obtained as a yellow-green powder. Yield: 99%. ^{1}H NMR (400 MHz, $CDCl_3$) δ/ppm = 8.55 (s, 1H), 7.87 (d, *J* = 8.0 Hz, 1H), 7.64 (d, *J* = 8.1 Hz, 1H), 7.45 (t, *J* = 7.8 Hz, 1H), 7.30 (d, *J* = 7.9 Hz, 1H), 6.14 (s, 1H), 3.35 (s, 3H), 3.15 (s, 3H). HRMS (ESI): calcd., $[M+H]^+$ = 344.0954, found: $[M+H]^+$ = 344.0954.

General procedure for the synthesis of ***BDB7*** *and* ***BDB8****.*

To a acetonitrile solution containing ***BDB1*** or ***BDB2*** (1.0 equiv.) was added aniline (2.0 equiv.) and K_2CO_3 (2.0 equiv.), and the resulting mixture was heated to reflux for 6 h. After cooling down to room temperature, the precipitation was filtered and rinsed with cold acetonitrile.

BDB7 was obtained as a light yellow powder. Yield: 76%. ^{1}H NMR (400 MHz, $CDCl_3$) δ/ppm = 8.37 (s, 1H), 8.20 (d, *J* = 5.6, 1H), 7.97 (d, *J* = 8.5, 1H), 7.74 (d, *J* = 7.9, 1H), 7.55 (dd, *J* = 16.3, 7.7, 3H), 7.42 (dt, *J* = 11.1, 7.5, 3H), 7.24 (d, *J* = 7.5, 1H), 6.84 (d, *J* = 5.6, 1H). HRMS (ESI): calcd., $[M+H]^+$ = 392.0954, found: $[M+H]^+$ = 392.0958.

BDB8 was obtained as an offwhite powder. Yield: 89%. ^{1}H NMR (400 MHz, d_6-DMSO) δ/ppm = 10.61 (s, 1H), 8.83 (s, 1H), 8.03 (d, *J* = 7.9, 1H), 7.73 (d, *J* = 8.0, 1H), 7.55 (t, *J* = 7.8, 3H), 7.40 (dd, *J* = 14.0, 6.1, 3H), 7.20 (s, 1H), 6.53 (s, 1H). HRMS (ESI): calcd., $[M+H]^+$ = 392.0954, found: $[M+H]^+$ = 392.0956.

Synthesis of ***Cys-BDB****.*

BDB1 or **BDB2** (0.075mmol), Cysteine (0.75 mmol) and NaOH (0.075 mmol) was dissolved in 55 mL of acetonitrile/water (10: 1, v/v). After stirring at room temperature for 12 h, the reaction mixture was poured into water, and the product was extracted with dichloromethane. The organic layer was dried over $MgSO_4$, concentrated to give **Cys-BDB** as yellow solid.

Cys-BDB1: Yield: 51%. ^{1}H NMR (400 MHz, d_6–DMSO) δ/ppm = 8.30 (d, *J* = 4.0 Hz, 1H), 8.07 (d, *J* = 7.9 Hz, 1H), 7.82 (d, *J* = 7.9 Hz, 1H), 7.59–7.44 (m, 3H), 6.69 (d, *J* = 4.0 Hz, 1H), 4.85 (s, 1H), 3.20–3.09 (m, 2H). HRMS (ESI): calcd., $[M+Na]^+$ = 442.0391, found: $[M+Na]^+$ = 442.0377.

Cys-BDB2: Yield: 65%. ^{1}H NMR data cannot be obtained due to its poor solubility. HRMS (ESI): calcd., $[M+Na]^+$ = 442.0391, found: $[M+Na]^+$ = 442.0364.

2. X-ray crystallographic analysis

BDB1. Yellow and prism single crystals of **BDB1** were grown from a solution of CH_2Cl_2. Intensity data were collected at 293 K on a Gemini A Single Crystal CCD X-ray diffractometer with $Mo_{K\alpha}$ radiation (l = 0.71073 Å) and graphite monochromator. The structure was solved by direct methods (SHELX-97) and refined by the full-matrix least-squares on F_2 (SHELX-97). All the non-hydrogen atoms were refined anisotropically and all the hydrogen atoms were placed by using AFIX instructions. Crystal data: $C_{13}H_6BClF_2N_4S$, *M*W = 334.54, Triclinic, *P* -1, *a* = 7.645(3), *b* = 8.842(3), *c* = 10.324(2) Å, α = 104.02(2)°, β = 94.76(2)°, γ = 100.91(3)°, V = 658.7(4) Å^3, Z = 2, D_{calc} = 1.687

mg/m^{-3}; μ = 4.285 mm^{-1}; R_1 ($I > 2\sigma(I)$) = 0.0878, wR_2 (all data) = 0.2512, GOF = 0.915. Total 3480 reflections were collected, among which 2294 reflections (199 parameters) were independent (R_{int} = 0.0572). CCDC-1470176.

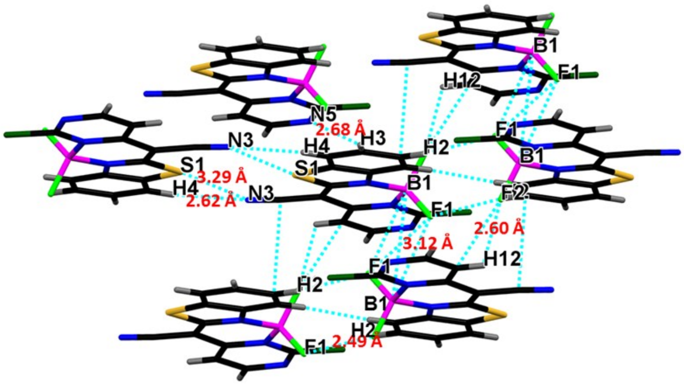

Fig. S1. Crystal packing structure of **BDB1**. The cyan dotted lines show intermolecular interactions within **BDB1**.

BDB2. Yellow and prism single crystals of ***BDB2*** were grown from a solution of CH_2Cl_2. Intensity data were collected at 293 K on a Gemini A Single Crystal CCD X-ray diffractometer with $Mo_{K\alpha}$ radiation (l = 0.71073 Å) and graphite monochromator. The structure was solved by direct methods (SHELX-97) and refined by the full-matrix least-squares on F_2 (SHELX-97). All the non-hydrogen atoms were refined anisotropically and all the hydrogen atoms were placed by using AFIX instructions. Crystal data: $C_{13}H_6BClF_2N_4S$, MW = 334.54, Triclinic, P -1, a = 9.628(9), b = 11.936(12), c = 12.293(12) Å, α = 100.080(12)°, β = 93.490(12)°, γ = 103.522(13)°, V = 1345(2) Å^3, Z = 4, D_{calc} = 1.652 mg/m^{-3}; μ = 0.1018 mm^{-1}; R_1 ($I > 2\sigma(I)$) = 0.3009, wR_2 (all data) = 0.3028, GOF = 1.137. Total 6760 reflections were collected, among which 4632 reflections (397 parameters) were independent (R_{int} = 0.0503). CCDC-1470180.

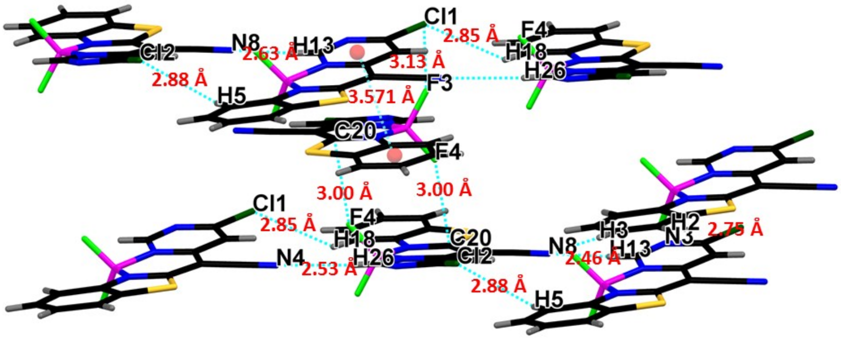

Fig. S2. Crystal packing structure of **BDB2**. The cyan dotted lines show intermolecular interactions within **BDB2**.

BDB3. Light yellow and prism single crystals of **BDB3** were grown from a solution of CH_2Cl_2. Intensity data were collected at 293 K on a Gemini A Single Crystal CCD X-ray diffractometer with $Mo_{K\alpha}$ radiation (l = 0.71073 Å) and graphite monochromator. The structure was solved by direct methods (SHELX-97) and refined by the full-matrix least-squares on F_2 (SHELX-97). All the non-hydrogen atoms were refined anisotropically and all the hydrogen atoms were placed by using AFIX instructions. Crystal data: $C_{14}H_9BF_2N_4OS$, MW = 330.12, Triclinic, P -1, a = 4.7639(7), b = 11.7169(19), c = 12.608(2) Å, α = 83.834(14)°, β = 86.891(13)°, γ = 87.700(13)°, V = 698.21(19) Å^3, Z = 2, D_{calc} = 1.570 mg/m^{-3}; μ = 2.368 mm^{-1}; R_1 ($I > 2\sigma(I)$) = 0.0850, wR_2 (all data) = 0.2286, GOF = 1.198. Total 3742 reflections were collected, among which 2482 reflections (209 parameters) were independent (R_{int} = 0.0798). CCDC-1470177.

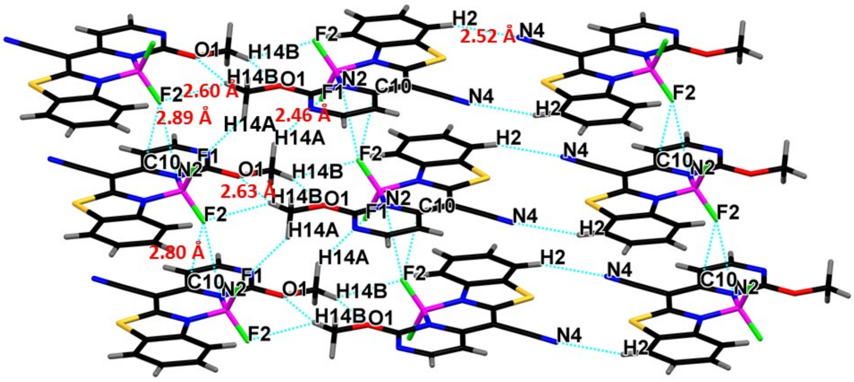

Fig. S3. Crystal packing structure of **BDB3**. The cyan dotted lines show intermolecular interactions within **BDB3**.

BDB4. Light yellow and prism single crystals of ***BDB*4** were grown from a solution of CH_2Cl_2. Intensity data were collected at 293 K on a Gemini A Single Crystal CCD X-ray diffractometer with Mo$_{K\alpha}$ radiation (l = 0.71073 Å) and graphite monochromator. The structure was solved by direct methods (SHELX-97) and refined by the full-matrix least-squares on F_2 (SHELX-97). All the non-hydrogen atoms were refined anisotropically and all the hydrogen atoms were placed by using AFIX instructions. Crystal data: $C_{14}H_9BF_2N_4OS$, MW = 330.12, Triclinic, P -1, a = 4.7955(5), b = 9.1763(13), c = 16.9010(17) Å, α = 100.887(10)°, β = 93.936(9)°, γ = 103.046(11)°, V = 706.67(15) Å^3, Z = 2, D_{calc} = 1.551 mg/m^{-3}; μ = 2.340 mm^{-1}; R_1 ($I > 2\sigma(I)$) = 0.0600, wR_2 (all data) = 0.2270, GOF = 0.687. Total 4168 reflections were collected, among which 2692 reflections (209 parameters) were independent (R_{int} = 0.0427). CCDC-1470181.

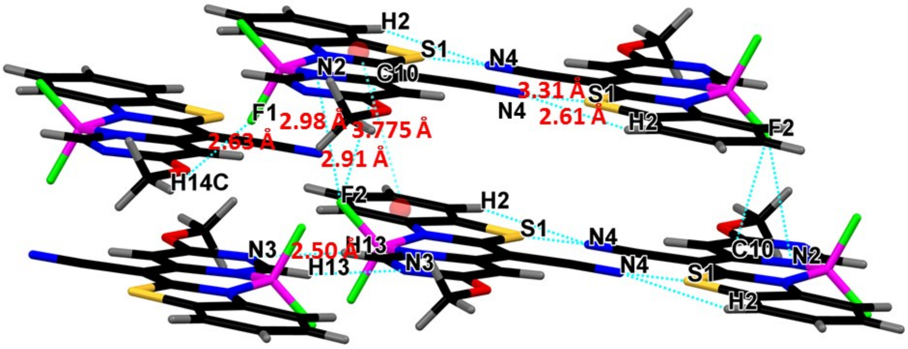

Fig. S4. Crystal packing structure of **BDB4**. The cyan dotted lines show intermolecular interactions within **BDB4**.

BDB5. Yellow and prism single crystals of ***BDB*5** were grown from a solution of CH_2Cl_2. Intensity data were collected at 293 K on a Gemini A Single Crystal CCD X-ray diffractometer with $Mo_{K\alpha}$ radiation (l = 0.71073 Å) and graphite monochromator. The structure was solved by direct methods (SHELX-97) and refined by the full-matrix least-squares on F_2 (SHELX-97). All the non-hydrogen atoms were refined anisotropically and all the hydrogen atoms were placed by using AFIX instructions. Crystal data: $C_{15}H_{12}BF_2N_5S$, MW = 343.17, Monoclinic, P 2(1)/c, a = 9.1073(8), b = 22.539(2), c = 7.3835(5) Å, α = 90°, β = 97.260(2)°, γ = 90°, V = 1503.4(2) Å^3, Z = 4, D_{calc} = 1.516 mg/m^{-3}; μ = 0.245 mm^{-1}; R_1 ($I > 2\sigma(I)$) = 0.0957, wR_2 (all data) = 0.3028, GOF = 1.083. Total 7139 reflections were collected, among which 2637 reflections (220 parameters) were independent (R_{int} = 0.0613). CCDC-1470214.

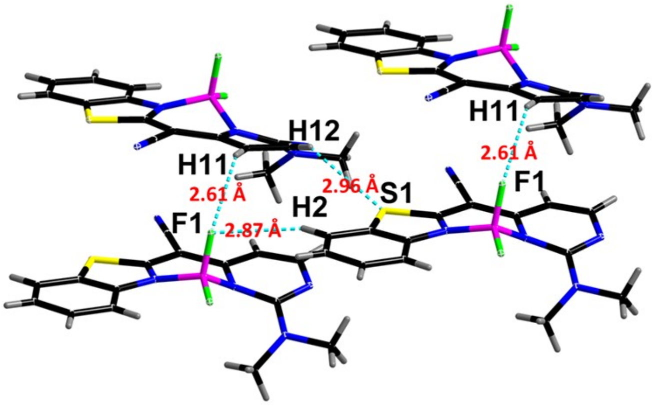

Fig. S5. Crystal packing structure of **BDB5**. The cyan dotted lines show intermolecular interactions within **BDB5**.

BDB6. Yellow and prism single crystals of ***BDB6*** were grown from a solution of CH_2Cl_2. Intensity data were collected at 293 K on a Gemini A Single Crystal CCD X-ray diffractometer with $Mo_{K\alpha}$ radiation (l = 0.71073 Å) and graphite monochromator. The structure was solved by direct methods (SHELX-97) and refined by the full-matrix least-squares on F_2 (SHELX-97). All the non-hydrogen atoms were refined anisotropically and all the hydrogen atoms were placed by using AFIX instructions. Crystal data: $C_{16}H_{13}BF_2N_4S$, MW = 342.17, Monoclinic, P 2(1)/c, a = 8.2568(7), b = 20.2980(17), c = 9.7220(9) Å, α = 90°, β = 113.857(8)°, γ = 90°, V = 1490.2(2) Å^3, Z = 4, D_{calc} = 1.525 mg/m^{-3}; μ = 2.187 mm^{-1}; R_1 ($I > 2\sigma(I)$) = 0.0557, wR_2 (all data) = 0.1437, GOF = 1.109. Total 8441 reflections were collected, among which 2600 reflections (220 parameters) were independent (R_{int} = 0.0613). CCDC-1470179.

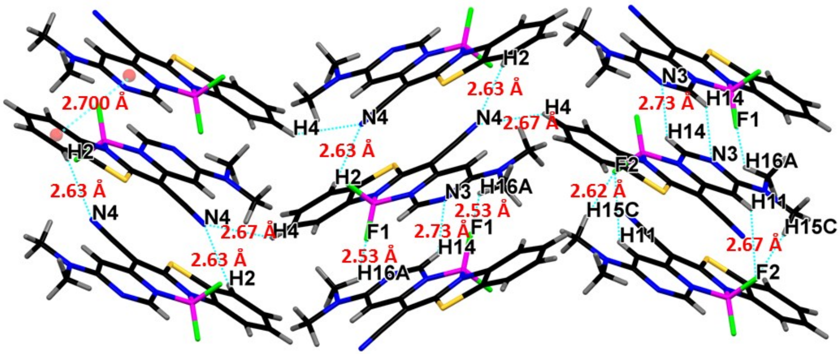

Fig. S6. Crystal packing structure of **BDB6**. The cyan dotted lines show intermolecular interactions within **BDB6**.

BDB7. Yellow and prism single crystals of ***BDB*7** were grown from a solution of CH_2Cl_2. Intensity data were collected at 293 K on a Gemini A Single Crystal CCD X-ray diffractometer with $Mo_{K\alpha}$ radiation (l = 0.71073 Å) and graphite monochromator. The structure was solved by direct methods (SHELX-97) and refined by the full-matrix least-squares on F_2 (SHELX-97). All the non-hydrogen atoms were refined anisotropically and all the hydrogen atoms were placed by using AFIX instructions. Crystal data: $C_{19}H_{12}BF_2N_5S$, *M*W = 391.21, Orthorhombic, *P b c a*, *a* = 7.1001(6), *b* = 41.434(3), *c* = 11.4739(7) Å, *α* = 90°, *β* = 90°, *γ* = 90°, V = 3375.4(5) Å^3, Z = 8, D_{calc} = 1.540 mg/m^{-3}; μ = 2.036 mm^{-1}; R_1 ($I > 2\sigma(I)$) = 0.0975, wR_2 (all data) = 0.2418, GOF = 1.083. Total 6772 reflections were collected, among which 3026 reflections (253 parameters) were independent (R_{int} = 0.0656). CCDC-1470182.

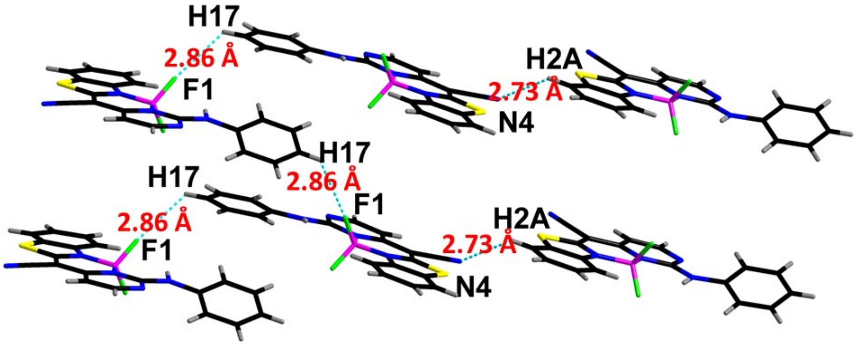

Fig. S7. Crystal packing structure of **BDB7**. The cyan dotted lines show intermolecular interactions within **BDB7**.

BDB8. Yellow and prism single crystals of ***BDB8*** were grown from a solution of CH_2Cl_2. Intensity data were collected at 293 K on a Gemini A Single Crystal CCD X-ray diffractometer with $Mo_{K\alpha}$ radiation (l = 0.71073 Å) and graphite monochromator. The structure was solved by direct methods (SHELX-97) and refined by the full-matrix least-squares on F_2 (SHELX-97). All the non-hydrogen atoms were refined anisotropically and all the hydrogen atoms were placed by using AFIX instructions. Crystal data: $C_{21}H_{18}BF_2N_5OS_2$, *M*W = 469.33, Triclinic, *P* -1, *a* = 9.9073(10), *b* = 11.0350(15), *c* = 11.0926(11) Å, *α* = 103.584(10)°, *β* = 95.854(9)°, *γ* = 113.279(11)°, V = 1056.7(2) Å^3, Z = 2, D_{calc} = 1.475 mg/m^{-3}; μ = 2.658 mm^{-1}; R_1 ($I > 2\sigma(I)$) = 0.0563, wR_2 (all data) = 0.1520, GOF = 1.024. Total 6345 reflections were collected, among which 3782 reflections (291 parameters) were independent (R_{int} = 0.0425). CCDC-1470183.

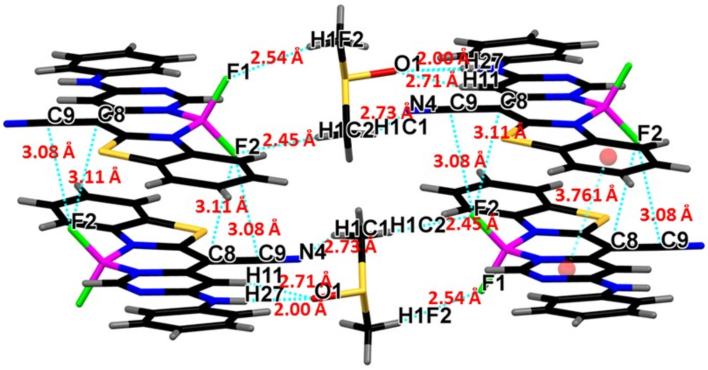

Fig. S8. Crystal packing structure of **BDB8**. The cyan dotted lines show intermolecular interactions within **BDB8**.

3. Absorption and emission spectra of BDB1–8 in different solvents

UV-vis absorption spectra were recorded on a Shimadzu UV-3600 spectrometer with a resolution of 1.0 nm. A solution of the sample (*ca.* 10^{-5} M) in a 1 cm square quarts cell was used for the measurement. Fluorescence spectra were recorded on a Hitachi F-7000 spectrometer. Powder samples of **BDB1-8** were used for the absorption and emission spectra recording. The fluorescence lifetimes and the absolute quantum yields (Φ_f) of the powder samples were determined with a Horiba Jobin Yvon Fluorolog-3 spectrofluorimeter. Fluorescence quantum yield of **BDB1-8** in solution were determined by using 4-methylamino-7-nitro-2,1,3-benzoxadiazole (Φ_f = 0.38 in acetonitrile) as reference.[2]

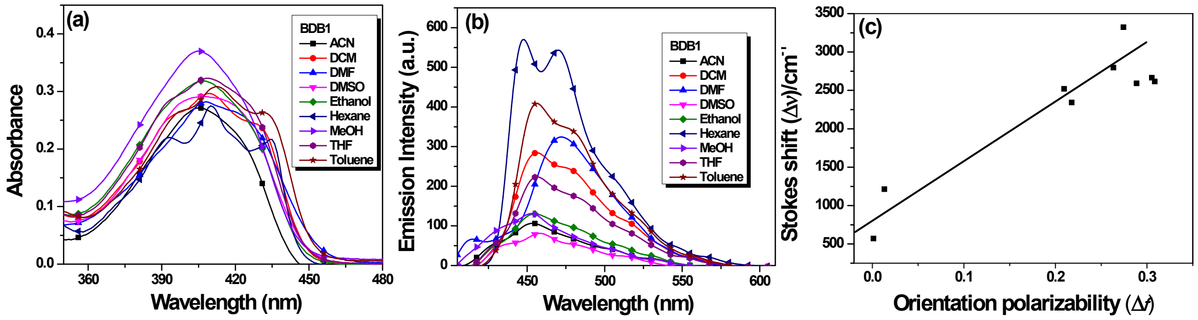

Fig. S9. Absorption (a), emission spectra (b) and the Lippert-Mataga plot (c) of **BDB1** in various solvents.

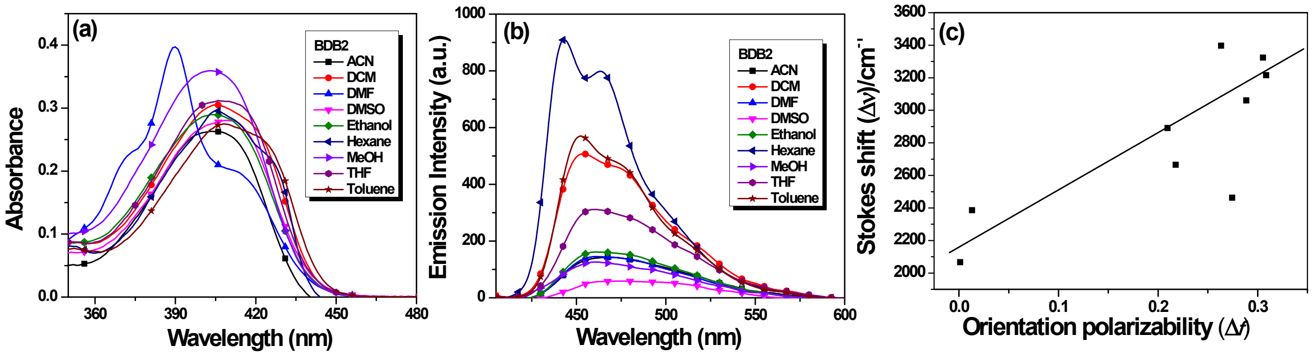

Fig. S10. Absorption (a), emission spectra (b) and the Lippert-Mataga plot (c) of **BDB2** in various solvents.

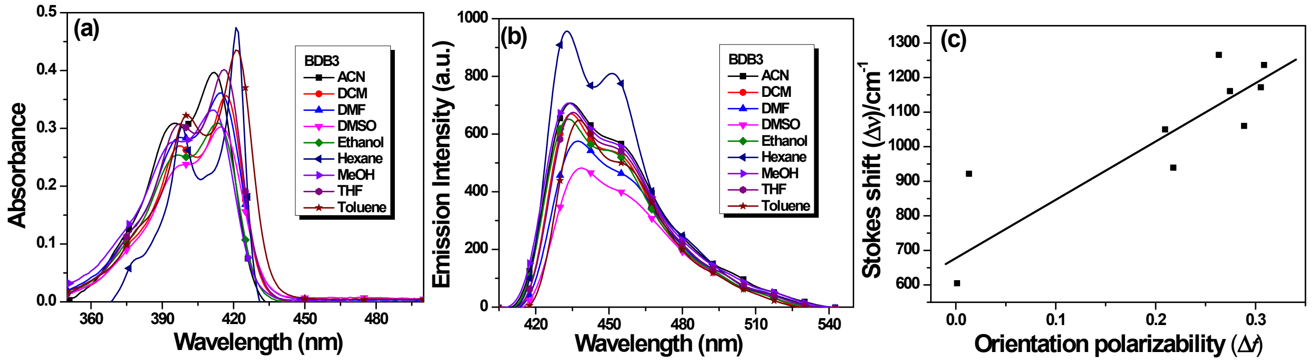

Fig. S11. Absorption (a), emission spectra (b) and the Lippert-Mataga plot (c) of **BDB3** in various solvents.

---

[2] S. Uchiyama, Y. Matsumura, A. P. de Silva, K. Iwai, *Anal. Chem.,* 2003, **75**, 5926.

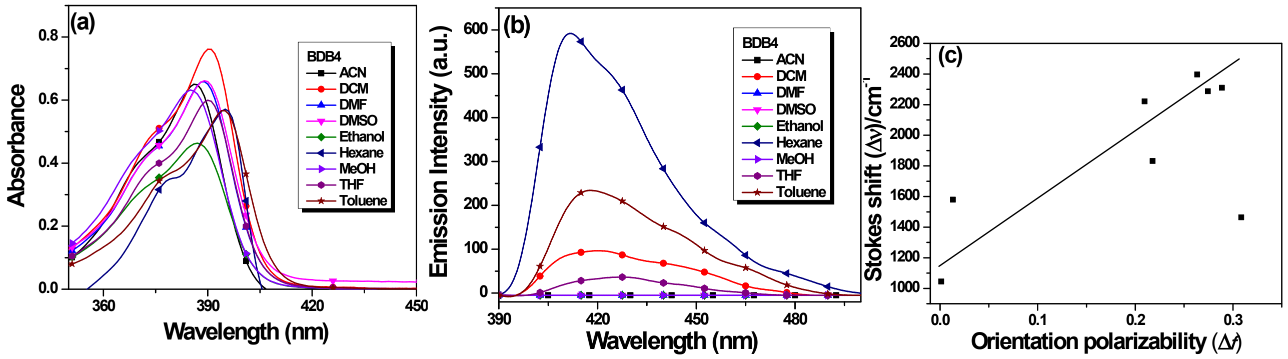

Fig. S12. Absorption (a), emission spectra (b) and the Lippert-Mataga plot (c) of **BDB4** in various solvents.

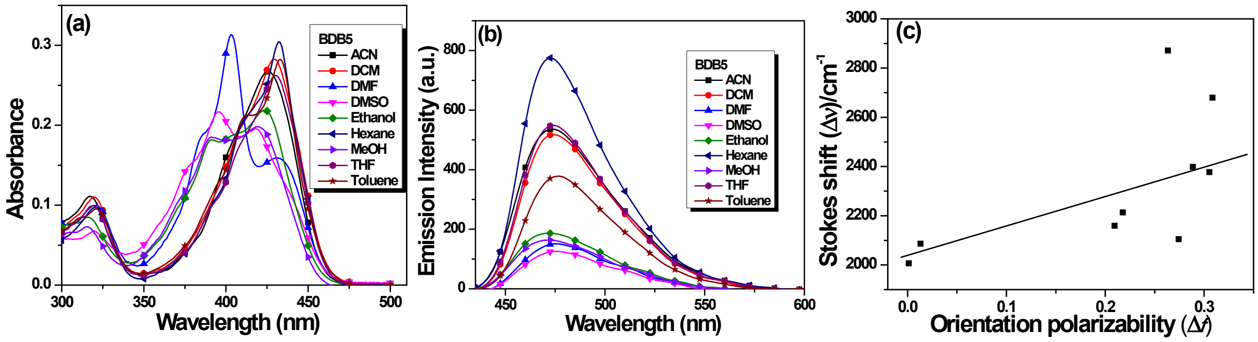

Fig. S13. Absorption (a), emission spectra (b) and the Lippert-Mataga plot (c) of **BDB5** in various solvents.

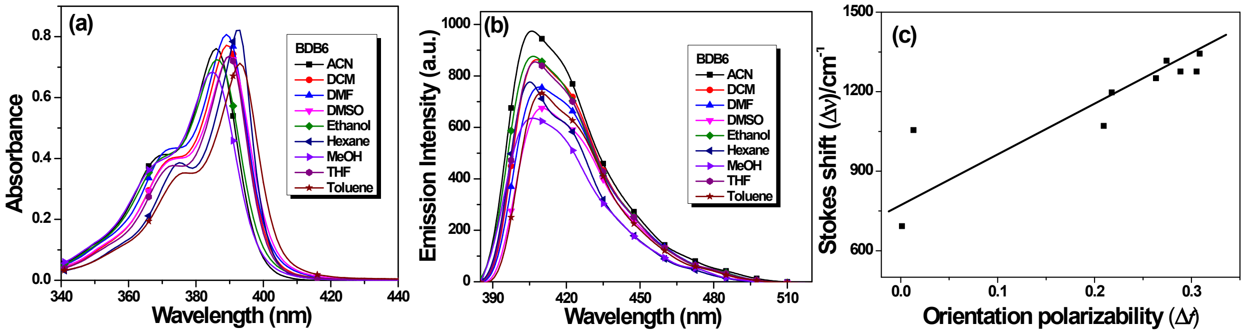

Fig. S14. Absorption (a), emission spectra (b) and the Lippert-Mataga plot (c) of **BDB6** in various solvents.

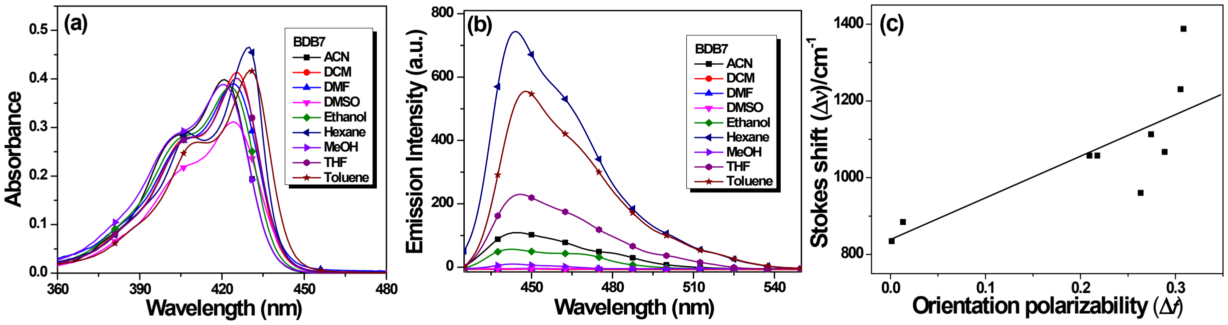

Fig. S15. Absorption (a), emission spectra (b) and the Lippert-Mataga plot (c) of **BDB7** in various solvents.

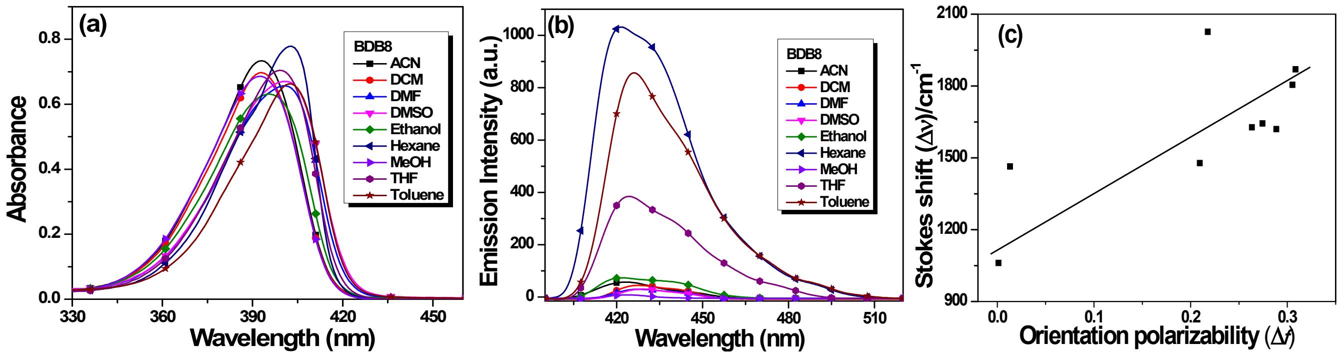

Fig. S16. Absorption (a), emission spectra (b) and the Lippert-Mataga plot (c) of **BDB8** in various solvents.

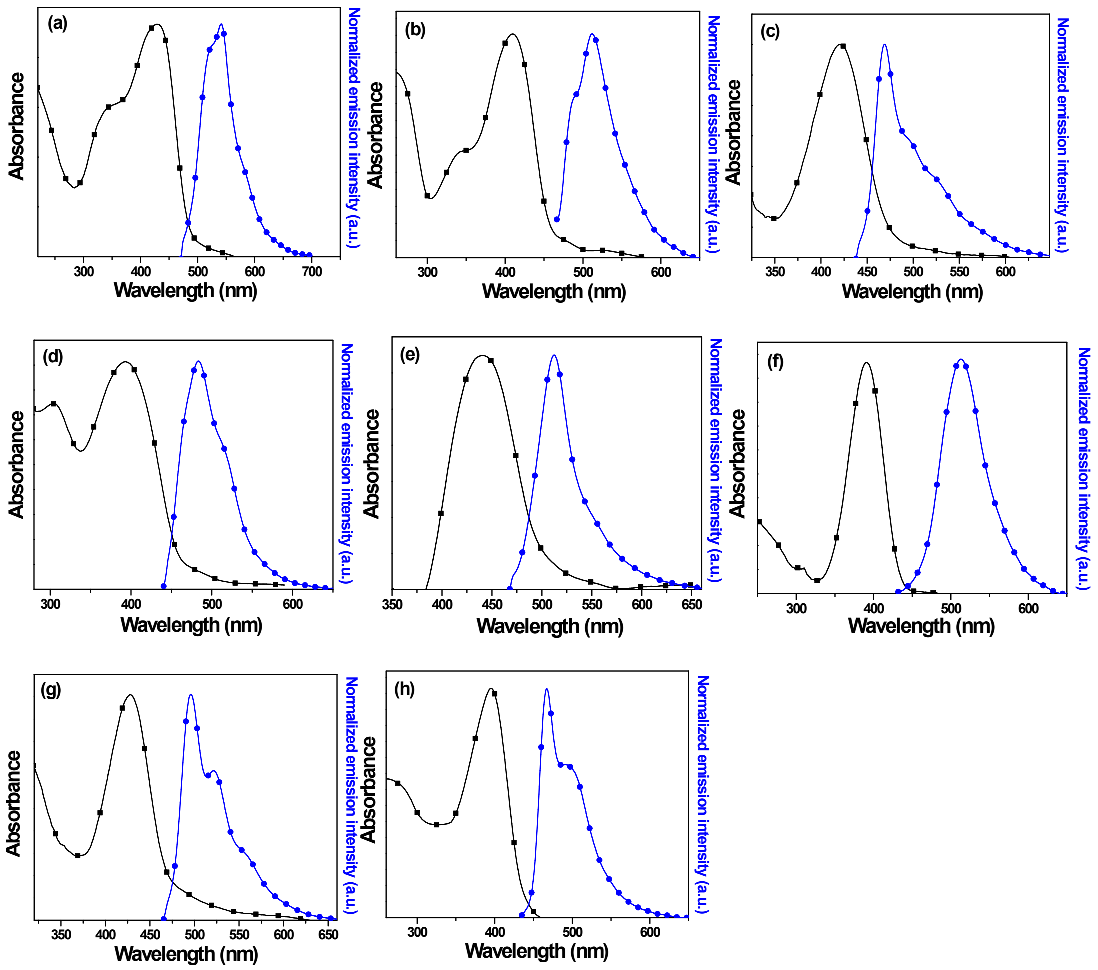

Fig. S17. Absorption and emission of **BDB1** (a), **BDB2** (b), **BDB3** (c), **BDB4** (d), **BDB5** (e), **BDB6** (f), **BDB7** (g) and **BDB8** (h) in the solid state.

4. Theoretical Calculations

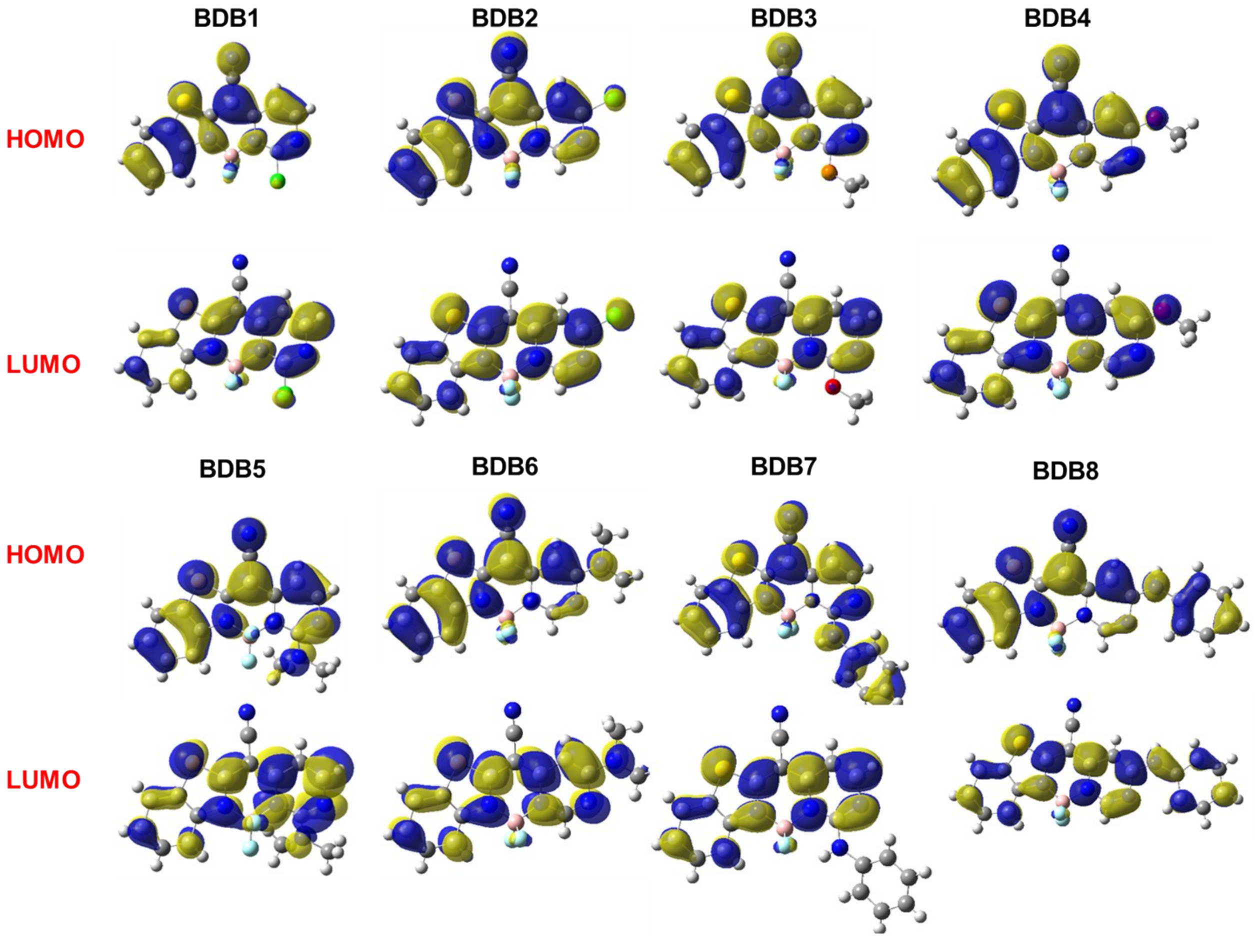

Fig. S18. Moldecular orbital amplitude plots of HOMOs and LUMOs of **BDB1–8** calculated by using B3LYP/6-31G+(d, p) basis set with G03 program.

5. Fluorescent Sensing of Cys.

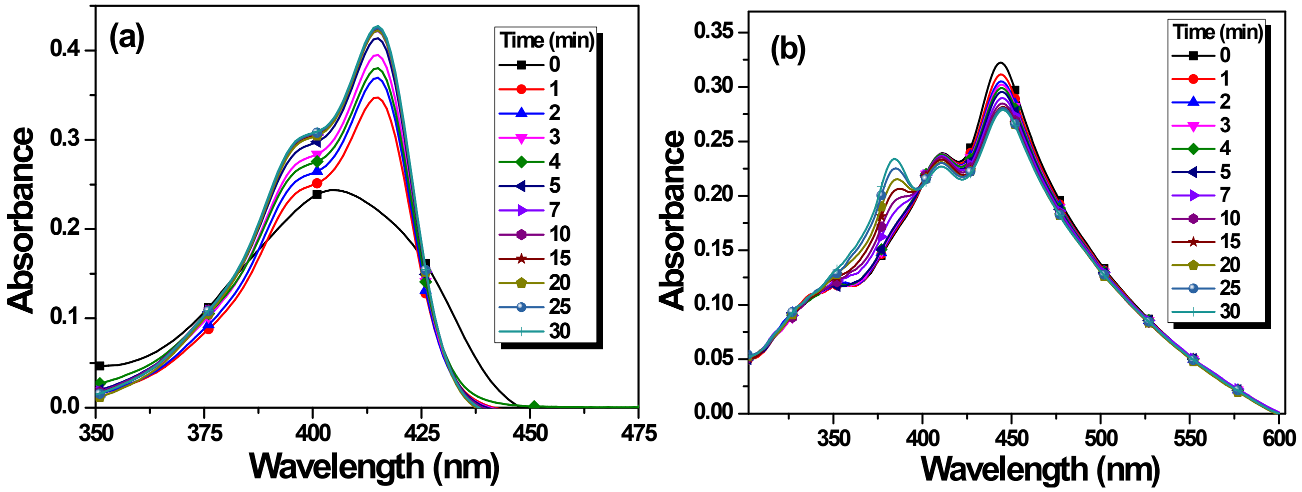

Fig. S19. Time-dependent absorption spectra of **BDB1** (a) and **BDB2** (b) (10 μM) with 100 equiv. of Cys in acetonitrile/HEPES buffer (15: 85, v/ v, 50 mM, pH 7.2) at 37 °C.

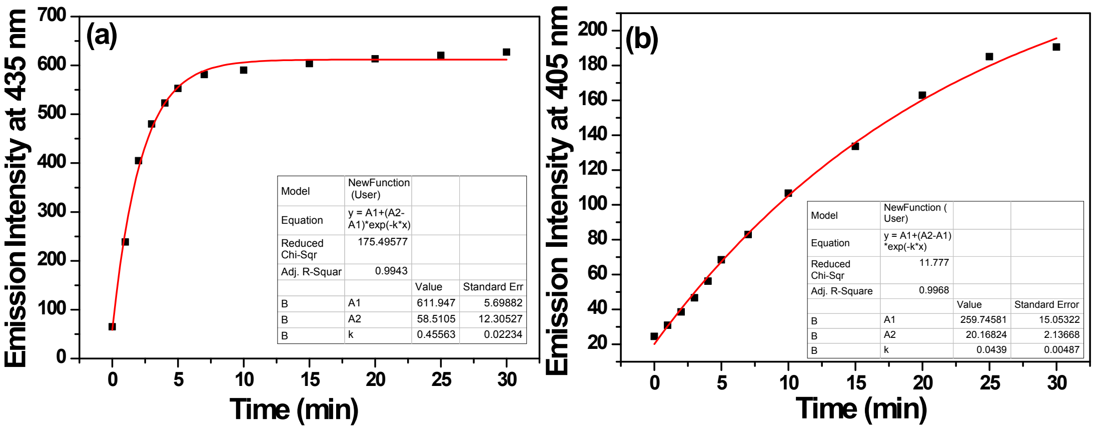

Fig. S20. Fluorescence kinetics of **BDB1** (a) and **BDB2** (b) (10 μM) upon addition of 1000 μM Cys in acetonitrile/HEPES buffer (15: 85 v/v, 50 mM, pH 7.2) at 37 °C. The reaction for **BDB1** and **BDB2** is monitored at 435 (λ_{ex} = 400 nm) and 405 nm (λ_{ex} = 385 nm), respectively. The data curve is fitted (red line) by a first order reaction scheme (see equation inserted, where A1 and A2 are the final and initial intensity, respectively. The observed pseudo-first-order rate constant k_{obs} were determined to be about 0.456 min^{-1} (**BDB1**) and 0.091 min^{-1}(**BDB2**).

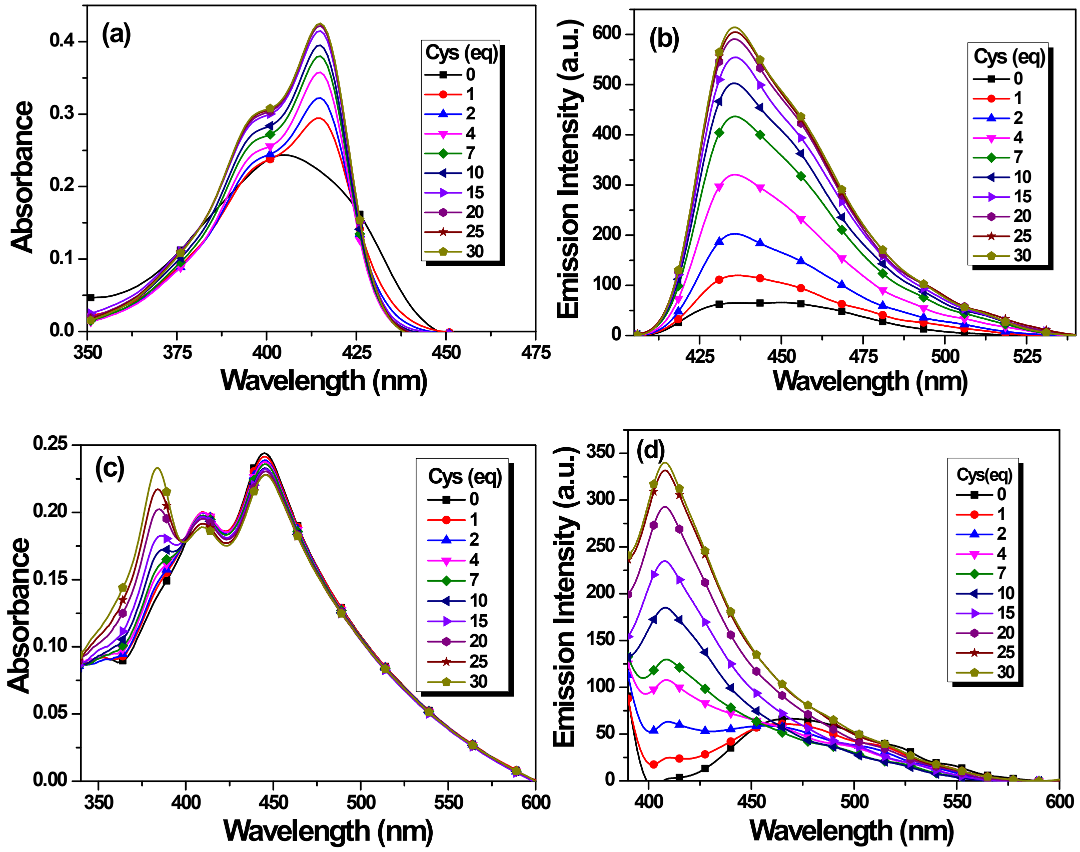

Fig. S21. Absorption and emission spectra of **BDB1** (a, b) and **BDB2** (c, d) (10 μM) upon addition of increasing concentrations of Cys (**BDB1:** λ_{ex} = 400 nm, slit width = d_{ex} = d_{em} = 2.5 nm, PMT voltage = 650 V; **BDB2**: λ_{ex} = 385 nm, slit width = d_{ex} = d_{em} = 5.0 nm, PMT voltage = 700 V) in acetonitrile/HEPES buffer (15: 85, v/v, 50 mM, pH 7.2) at 37 °C. Each spectrum was acquired 1 h after Cys addition.

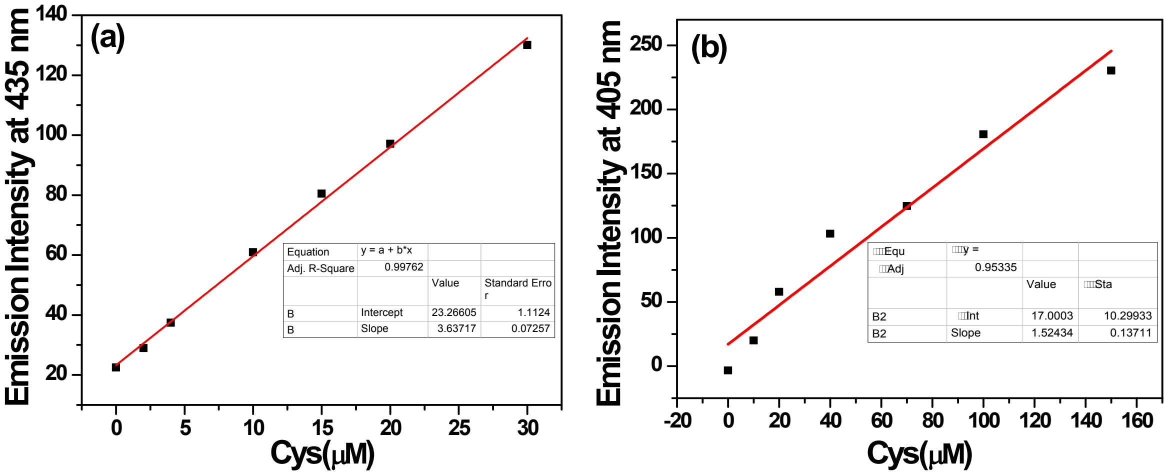

Fig. S22. Plot of fluorescence intensity of **BDB1** (a) and **BDB2** (b) (10 μM) at 435 and 405 nm in acetonitrile/HEPES buffer (15: 85, v/ v, 50 mM, pH 7.2) at 37 °C as a function of Cys concentration in the range of 0-30 μM and 0-150 μM, respectively. The detection limit (3σslope^{-1}) was then determined to be 268 and 642 nM, respectively.

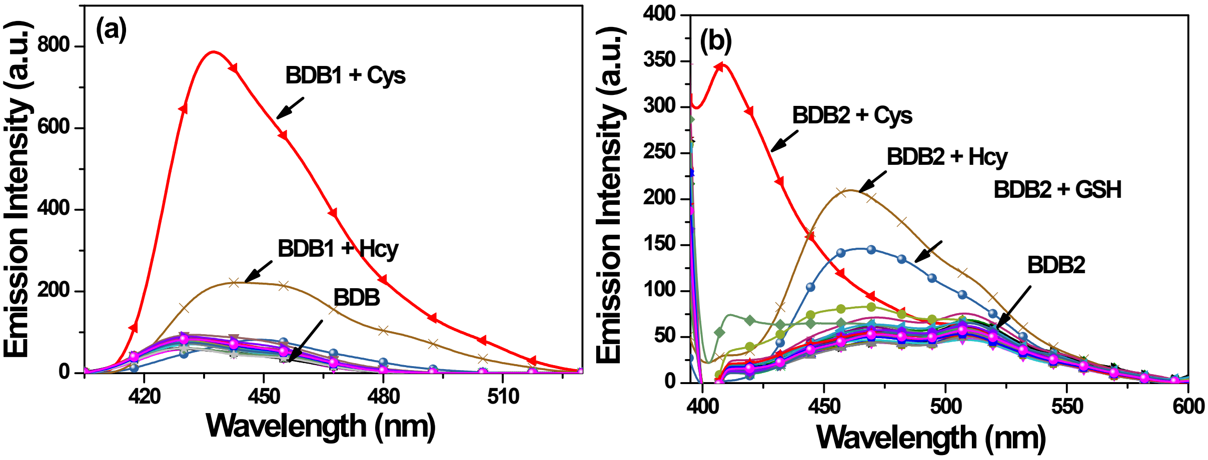

Fig. S23. Emission spectra of **BDB1** (a) and **BDB2** (b) upon addition of 1000 μM physiological important amino acids in acetonitrile/HEPES buffer (15: 85, v/v, 50 mM, pH 7.2) at 37 °C.

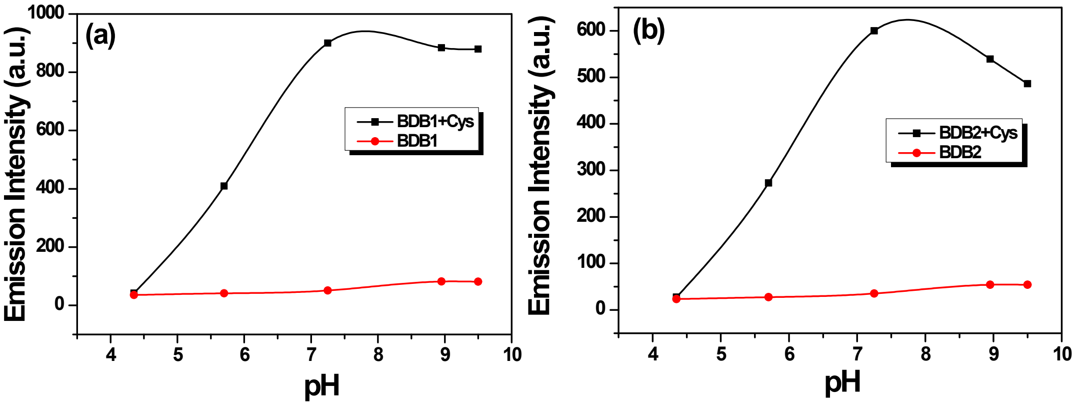

Fig. S24. Effects of pH on the emission of **BDB1** (a) at 435 nm and **BDB2** (b) at 405 nm (10 μM) reacting with Cys (100 μM).

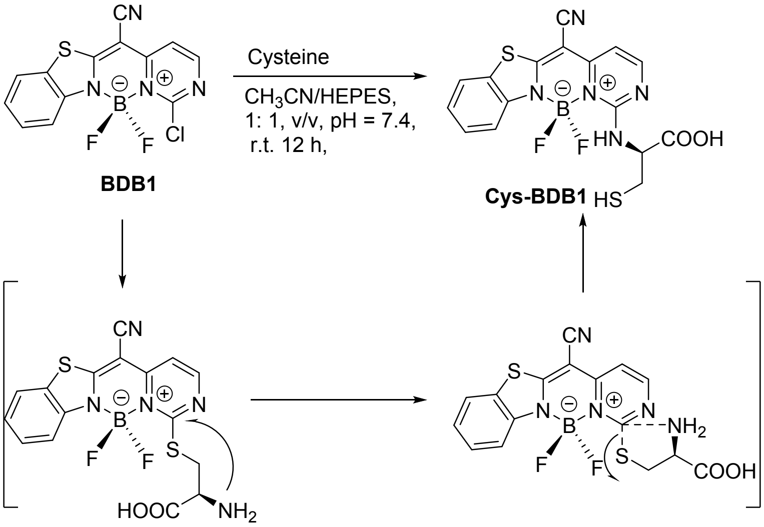

Scheme S1. Proposed mechanism of **BDB1** for highly selective sensing of Cys.

6. Cell culture methods and confocal imaging

HeLa cells were cultured in Dulbecco’s Modified Eagle Medium supplemented with 10% fetal bovine serum, penicillin (100 units/mL), streptomycin (100 mg/mL) and 5% CO_2 at 37 °C. After removing the incubation media and rinsing with 1× PBS for three times. The cells were treated with N-methylmaleimide (1 mm) in culture media for 20 min at 37 °C , and then washed with D-Hanks. The cells were further stained with **BDB1** solution (20 μM, in 1 × PBS containing 0.1% DMSO) for 30 h at 25 °C. Then the cells were washed three times with **BDB1** and imaged with Zeiss LSM-710 microscope equipped with a 60× oil-immersion objective. The images were obtained upon irradiation at 405 nm with a band path from 420-480 nm.